Parallel tempering Monte Carlo simulations of lysozyme orientation on charged surfaces

Yun Xie, Jian Zhou, and Shaoyi Jiang

Citation: The Journal of Chemical Physics **132**, 065101 (2010); doi: 10.1063/1.3305244
View online: http://dx.doi.org/10.1063/1.3305244
View Table of Contents: http://scitation.aip.org/content/aip/journal/jcp/132/6?ver=pdfcov
Published by the AIP Publishing

Parallel tempering Monte Carlo simulations of lysozyme orientation on charged surfaces

Yun Xie,[1] Jian Zhou,[1,a)] and Shaoyi Jiang[2]
[1]*Guangdong Provincial Key Lab for Green Chemical Product Technology, School of Chemistry and Chemical Engineering, South China University of Technology, Guangzhou, Guangdong 510640, People's Republic of China*
[2]*Department of Chemical Engineering, University of Washington, Seattle, Washington 98195, USA*

(Received 30 July 2009; accepted 12 January 2010; published online 9 February 2010)

In this work, the parallel tempering Monte Carlo (PTMC) algorithm is applied to accurately and efficiently identify the global-minimum-energy orientation of a protein adsorbed on a surface in a single simulation. When applying the PTMC method to simulate lysozyme orientation on charged surfaces, it is found that lysozyme could easily be adsorbed on negatively charged surfaces with "side-on" and "back-on" orientations. When driven by dominant electrostatic interactions, lysozyme tends to be adsorbed on negatively charged surfaces with the side-on orientation for which the active site of lysozyme faces sideways. The side-on orientation agrees well with the experimental results where the adsorbed orientation of lysozyme is determined by electrostatic interactions. As the contribution from van der Waals interactions gradually dominates, the back-on orientation becomes the preferred one. For this orientation, the active site of lysozyme faces outward, which conforms to the experimental results where the orientation of adsorbed lysozyme is co-determined by electrostatic interactions and van der Waals interactions. It is also found that despite of its net positive charge, lysozyme could be adsorbed on positively charged surfaces with both "end-on" and back-on orientations owing to the nonuniform charge distribution over lysozyme surface and the screening effect from ions in solution. The PTMC simulation method provides a way to determine the preferred orientation of proteins on surfaces for biosensor and biomaterial applications.
 [doi:10.1063/1.3305244]

I. INTRODUCTION

Protein adsorption plays an important role not only in many fundamental biological phenomena,[1,2] but also in many biotechnological applications,[3–7] such as biosensors, protein separation, drug delivery, biocatalyst, artificial biomaterials, etc. Among these applications, proper adsorbed protein orientation is a key issue for the performance of biosensors, biocatalyst, and biomaterials because protein orientation will affect the accessibility of the active site of enzyme[8] or the antigen recognition site of antibody.[9]

Protein adsorption has been widely studied by theoretical, experimental, and computer simulation approaches.[10–19] It is generally accepted that surface-induced conformational change is much slower than orientational change on surfaces,[13,20] suggesting that proteins initially undergo translational and rotational motions to tether onto the surface with preferred orientation before the following conformational changes to occur. Therefore, in simulations of protein adsorption, it is efficient to first determine the preferred protein orientation on surfaces before molecular dynamics (MD) simulations are carried out to investigate the adsorption-induced conformational change in proteins. As commented by Trzaskowski *et al.*,[21] the most complete approach[22,23] uses Monte Carlo (MC) simulation to determine the most probable orientation of adsorbed protein on surface, and this orientation serves as the initial orientation in the subsequent MD simulation to study the conformational change after adsorption. There are two common ways to determine the initial orientation in MD simulation. One is simply to select random or specific orientations as initial orientations. Another is to adopt energy-based methods[22,24–26] which are more frequently used now and are more reliable. They are based on a thermodynamic energy equation coupled with designated configuration space sampling techniques to identify the lowest-energy (global-minimum-energy) orientation.

However, in the energy-based method to probe possible orientations of adsorbed protein, one awkward problem encountered is the representativeness of configuration space sampling. Conventional MC and MD simulations in canonical ensemble often suffer from the quasiergodicity problem, i.e., simulations at low temperatures tend to get trapped in local-minimum-energy states and thus fail to sample the whole configuration space. Therefore, when Metropolis MC simulation is applied to probe lowest-energy orientation, dozens of independent MC simulations are often performed to explore possible orientations, and then the lowest-energy orientation is identified from these possible orientations. This process is not only time consuming, but may also be unreliable, since each individual simulation might become trapped in a local-minimum-energy state and the global-minimum-energy state may never be sampled. To improve the effi-

[a)]Author to whom correspondence should be addressed. Tel.: +86-20-87114069. FAX: +86-20-87114069. Electronic mail: jianzhou@scut.edu.cn.

ciency of configuration space sampling, various algorithms[27–37] have been proposed by performing molecular simulation in generalized ensemble based on non-Boltzmann probability distribution [e.g., multicanonical algorithms[27] and simulated tempering[28] or improving updates of configurations in numerical simulation (e.g., cluster algorithm,[29] parallel tempering,[30] also replica exchange)]. Among these algorithms, parallel tempering, first introduced in spin glass systems by Swendsen and Wang[30] and later applied in biological system by Hansmann,[31] is a promising method to improve the representativeness of sampling by exchanging configurations between replicas. There have been considerable improvements and extensions made to the algorithm,[32] such as performing parallel tempering in various ensembles[33–35] and in different parameter space,[33,36] or combining parallel tempering with other simulation methods.[37–41] de Pablo and co-workers proposed parallel tempering simulations in grand canonical ensemble[33] and multicanonical ensemble.[35] They also successfully combined extended ensemble density of states methods with parallel tempering to extensively sample configuration space and applied the method to study protein folding.[37–41]

Another problem encountered in the simulation of protein orientation is the computational expense. An atomistic model contains precise details of the structural information of a simulated system, and thus requires considerable computational resources, while a colloidal model is fast but might lose necessary structural details. So often a compromise should be made between the accuracy of a structural model and the efficiency of simulation. To reduce the computational expense as much as possible under the premise of adequate accuracy, appropriate coarse-grained models[25,42,43] are often employed. Residue model, representing each amino acid residue as one or a few interaction sites, retains the sequence information of protein well and thus could be used to predict the native structure of proteins and has showed its efficiency in molecular simulation of orientation of adsorbed proteins.[25]

Parallel tempering algorithm can be combined with MD or MC method. However, since a parallel tempering exchange is an unphysical move, one is doing a form of sampling of phase space rather than doing real dynamics, so one cannot draw conclusions about dynamics.[32] Compared with MD, MC is more efficient in phase space sampling since MC need not to follow a realistic path to obtain the correct equilibrium distribution and thus, in principle, can make large changes to configuration rapidly. In the molecular simulation of biological systems, parallel tempering algorithm has been used to investigate the stability of proteins on surfaces.[40,41,44] For example, Knotts *et al.*[41,44] successfully applied a method combining density-of-states based technique and parallel tempering to study the thermal stability and unfolding of proteins on surfaces.

In this work, to accurately and efficiently identify the lowest-energy orientation of adsorbed proteins on surfaces in a single simulation, a parallel tempering Monte Carlo (PTMC) algorithm is applied to investigate the protein orientation by a united-residue model. Lysozyme, a basic protein of low molecular weight with ellipsoid shape, has long been used as a model protein to study the enzyme kinetics, spatial conformation, and molecular immunology. Also, abundant experimental data of lysozyme adsorption are available.[45–49] Therefore in this work, lysozyme is chosen as the model protein so that simulation results could be compared with experimental data.

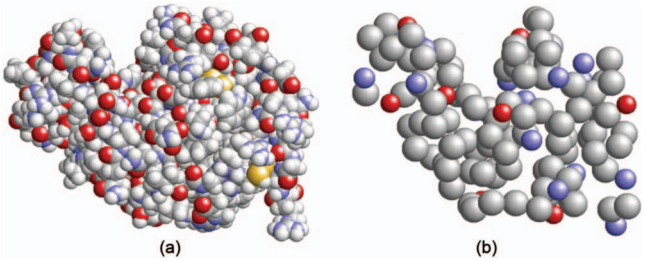

FIG. 1. Structural models of lysozyme. (a) Atomistic model. (b) Residue model.

II. METHODS

A. Models and force field

The crystal structure of lysozyme in Fig. 1(a) is taken from Protein Data Bank (PDB) and the PDB code of lysozyme is 1HEL. For a united-residue model[25] of protein, each amino acid is reduced to a sphere centered at α-carbon of the residue, in which the basic structure information of a protein is well kept, the residue-model structure of lysozyme is shown in Fig. 1(b).

The potential energy of protein-surface interaction (U_{tot}) is comprised of van der Waals (vdW) interaction energy (U_{vdW}) and electrostatic interaction energy (U_{ele}),

$$U_{\mathrm{tot}} = U_{\mathrm{vdW}} + U_{\mathrm{ele}}. \tag{1}$$

vdW interaction energy is calculated with Lennard-Jones potential model

$$U_{\mathrm{vdW}} = \varepsilon\left[\left(\frac{\sigma}{r}\right)^{12} - 2\left(\frac{\sigma}{r}\right)^{6}\right], \tag{2}$$

where ε is the energy at the pair minimum and σ is the distance at the minimum of the potential. Details of the coarse-grained force field interactions are the same as used in our previous work.[25]

The highly polar medium water is represented by an implicit solvent model in which the effect of solvent is accounted by a distance-dependant dielectric function[50]

$$U_{\mathrm{ele}} = \frac{\sigma_s q_i e^{-\kappa z}}{\kappa \varepsilon_0 \varepsilon_r}, \tag{3}$$

where z is the distance between one residue, and the surface σ_s is the surface charge density (SCD), q_i is the charge of one residue, κ is the inverse Debye length calculated by $1/\kappa = 0.304/\sqrt{\mathrm{I}}$ for a 1:1 salt, I is the ionic strength (IS), ε_0 is the permittivity of free space, and ε_r is the relative permittivity, which is assumed to be distance dependant: $\varepsilon_r = r$.

B. Simulation details

In parallel tempering simulations, N noninteracting replicas, each in canonical ensemble, are simultaneously simulated by distributing different replicas with different temperatures over N processes (one cluster node can have several processes). After a fixed number of MC moves, configurations between neighboring replicas (i.e., replica T_i and replica T_{i+1}) are swapped with the acceptance probability

$$p(E_i,T_i \rightarrow E_{i+1},T_{i+1}) = \min(1,\exp(\Delta\beta\Delta E)), \quad (4)$$

where

$$\Delta\beta = \frac{1}{k_B}\left(\frac{1}{T_{i+1}} - \frac{1}{T_i}\right)$$

is the difference between the inverse temperatures of neighboring replicas, and $\Delta E = E_{i+1} - E_i$ is the energy difference of neighboring replicas.

In each replica, regular MC simulations in canonical ensemble were carried out in a box of $10 \times 10 \times 10$ nm^3. Only one lysozyme molecule was considered in simulations. Initially, the lysozyme was put 5 nm above the surface with a random orientation. During simulations, the protein was translated and rotated around its center of mass. The displacement of each move was adjusted to ensure an acceptance ratio of 0.5. 20×10^6 MC cycles were carried out with 10×10^6 cycles for equilibrium and another 10×10^6 cycles for production.

In parallel tempering algorithm, the number of replicas and temperature distribution is of great importance to the efficiency and accuracy of simulations. Generally, the lowest temperature is often set to the interested one; the highest temperature should be high enough to ensure that simulation will not be trapped in local-minimum-energy states. There should be sufficient energy overlap between neighboring replicas to allow for the acceptance of configuration swaps. Some algorithms[51–53] have been proposed to achieve an optimal allocation of replicas and reasonable acceptance possibility. In our simulated system, five replicas were set with the temperature distribution of {310, 500, 800, 1500, and 2500 K}. All simulations were carried out on 64 bit Itanium cluster at SCUTGrid. To focus on the effect of electrostatic interactions on the orientation of protein adsorption, we investigated protein adsorption on charged surfaces at different ISs.

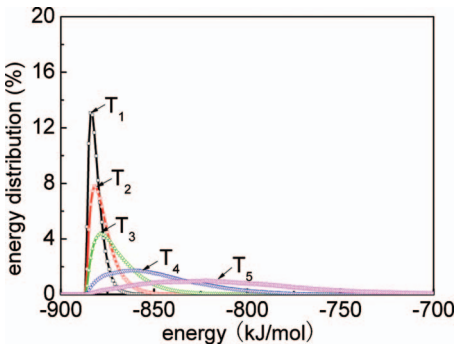

FIG. 2. Energy distribution of lysozyme adsorbed on a negatively charged surface with SCD=−0.018 C m^{-2} and IS=0.005 M. Replicas are labeled as $T_1, T_2, \ldots, T_5$.

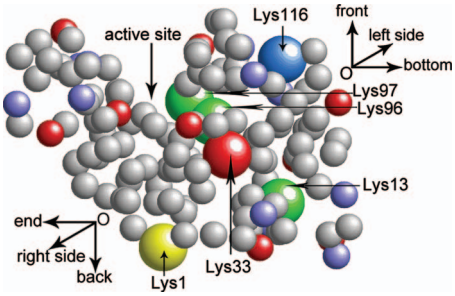

FIG. 3. Graphical elucidation for different parts of lysozyme.

Figure 2 shows the overlap of energy distribution of lysozyme adsorbed on a negatively charged surface with SCDs of −0.018 C m^{-2} and IS of 0.005 M. As shown in Fig. 2, the energy overlaps between neighboring replicas are sufficient to allow swaps. Situations under other conditions are similar and not shown here.

III. RESULTS AND DISCUSSION

Previous works[25,54,55] showed that electrostatic interactions play an important role in protein orientation on surfaces. In this work, we investigated lysozyme adsorption on both positively charged and negatively charged surfaces at different ISs. To quantitatively characterize the orientation of adsorbed proteins on surfaces, an orientation angle (θ) is employed and cos θ is calculated for each possible orientation. The orientation angle is defined as the angle between the unit vector normal to the surface and the unit vector along the dipole of a protein. To provide a clear picture of lysozyme orientation, different parts of lysozyme are labeled, as shown in Fig. 3. Lysine residues are also labeled for later elucidation of lysozyme orientation.

A. Performance comparison of PTMC to serial MC simulations

To compare the performance of PTMC simulation with that of conventional serial MC simulation, dozens of independent serial MC runs were carried out with the same parameters as in PTMC simulation. Figure 4 shows the orientation distribution of lysozyme adsorption on a negatively

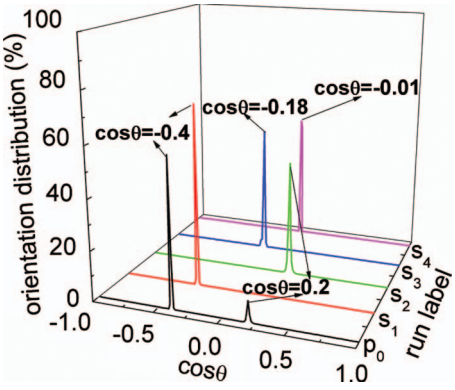

FIG. 4. Orientation distributions of lysozyme adsorbed on a negative surface at IS=0.02 M by PTMC and serial MC simulations. PTMC run is labeled as p_0 for comparison, and four different orientation distributions by serial MC runs are labeled as s_1, s_2, s_3, and s_4.

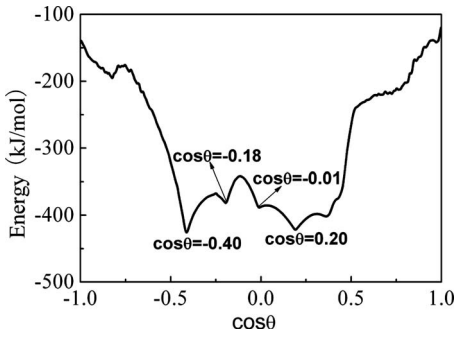

FIG. 5. Energy landscape of lysozyme adsorbed on a negatively charged surface at IS=0.02 M as a function of lysozyme orientation.

charged surface at IS of 0.02 M by serial MC runs. Four orientations sampled by serial MC runs were found, labeled as s_1, s_2, s_3, and s_4. The PTMC run with the same parameters is labeled as p_0 for comparison. Figure 5 displays the energy landscape of lysozyme adsorbed on a negatively charged surface at IS of 0.02 M as a function of orientation, with the orientations detected in simulations labeled.

From Fig. 4, it can be found that with dozens of serial MC runs carried out, the global-minimum-energy orientation ($\cos\theta=-0.4$) and another orientation that has close energy ($\cos\theta=0.2$) might be detected, but other orientations (e.g., $\cos\theta=-0.18$ or $\cos\theta=-0.01$) might also be sampled as preferred orientations if MC run traps in local-minimum-energy states. Therefore, when one obtains the lowest-energy orientation by comparing the energy of possible orientations sampled from serial MC simulations, there is no guarantee that the sampled orientation is the global-minimum-energy orientation because every serial MC run may trap in local-minimum-energy state. Furthermore, the orientation distribution could not be obtained in a single run by serial MC because of an incomplete configuration space sampling.

By contrast, the PTMC simulation could easily get out of local-minimum-energy states and sample all possible orientations from configuration space. The orientation distribution could also be acquired in a single simulation. From the statistic orientation distribution by PTMC simulation (Fig. 4), different possible orientations are identified according to the peaks of the orientation distribution curve and the most probable orientation (also preferred orientation) of the adsorbed protein is represented by the highest peak.

B. Lysozyme orientation on a negatively charged surface

Figure 6 shows the effect of IS on lysozyme orientation on a negatively charged surface (SCD=−0.018 C m^{-2}). When IS is low (0.005 M), lysozyme is adsorbed on the negatively charged surface with the preferred orientation of $\cos\theta=-0.4$ ("side-on" orientation), as shown in Fig. 7(a). When IS is 0.02 M, the "back-on" orientation with $\cos\theta=-0.4$ [Fig. 7(b)] starts to come up. When IS further increases to the physiological condition (~0.1 M), the back-on orientation becomes the preferred orientation. Meanwhile, as IS increases, the orientation distribution becomes wider, i.e., the number of possible orientations increases.

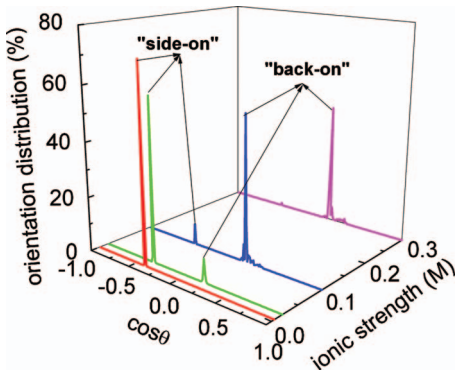

FIG. 6. Orientation distributions of lysozyme adsorbed on a negatively charged surface at different ISs.

Table I lists the averaged total adsorption potential energy of lysozyme (U_{av}), the total potential energy (U_{tot}), vdW potential energy (U_{vdW}), electrostatic potential energy (U_{ele}), and the percentage (P) of major lysozyme orientations adsorbed on a negatively charged surface. It is clear that the positively charged lysozyme could easily be adsorbed on an oppositely charged surface due to attractive electrostatic interactions. When solution IS is low (0.005 or 0.02 M), driven by dominant electrostatic interactions, lysozyme tends to be adsorbed on the negatively charged surface with side-on orientation. When the IS increases up to 0.1 or 0.3 M, owing to the screening effect of ions from solution, the energy contribution from electrostatic interactions to total potential energy gradually declines while that from vdW interactions increases, which leads to the change in preferred orientation from side-on to back-on.

Experimentally, binding orientations, especially detailed binding regions of proteins on surfaces, are rarely directly observed yet limited to the resolution of instruments.[13] How-

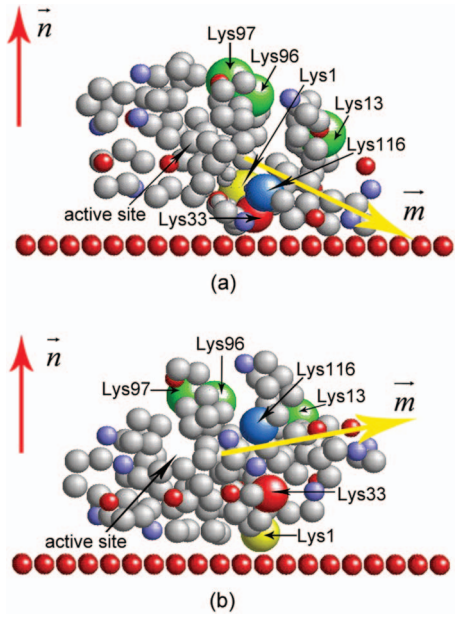

FIG. 7. Configurations of lysozyme orientation on a negatively charged surface. The direction of normal to surface is noted as $\vec{n}$ and the direction of dipole of lysozyme is noted as $\vec{m}$. (a) Side-on orientation ($\cos\theta=-0.4$); (b) back-on orientation ($\cos\theta=0.2$).

TABLE I. Energies and orientations of lysozyme adsorbed on a negatively charged surface.

IS (M)	U_{av} (kJ mol^{-1})	U_{tot} (kJ mol^{-1})	U_{vdW} (kJ mol^{-1})	U_{ele} (kJ mol^{-1})	cos θ	Orientation	P (%)	Fig.
0.005		−886.3	−70.6	−815.7	−0.40	Side-on	99.97	7(a)
	−886.3							
		−866.3	−72.0	−794.3	0.20	Back-on	0.03	7(b)
0.02		−426.3	−72.4	−354.0	−0.40	Side-on	91.04	7(a)
	−425.8							
		−420.6	−71.6	−349.0	0.20	Back-on	8.96	7(b)
0.1		−192.0	−68.3	−123.6	0.20	Back-on	95.71	7(b)
	−191.6							
		−184.3	−70.3	−113.9	−0.40	Side-on	4.29	7(a)
0.3	−124.1	−124.3	−71.9	−52.4	0.20	Back-on	97.83	7(b)
		−114.9	−69.9	−45.0	−0.40	Side-on	2.17	7(a)

ever, with special techniques, it is possible to infer binding regions of protein from experimental data. Dismer and Hubbuch[56,57] developed an effective lysine labeling technique to examine the binding orientations of lysozyme on ion-exchange adsorbents. They found that the binding sites of lysozyme are located around Lys1, Lys33, and Lys116. For side-on orientation predicted in our simulations [Fig. 7(a)], the active site faces sideways; there are two binding sites on the right side: one is between Lys1 and Lys33, and another between Lys33 and Lys116, whereas Lys13, Lys96, and Lys97 on the left side are exposed to solution. This simulation result agrees well with the experimental results by Dismer *et al.*[56,57] of lysozyme adsorption on strongly negatively charged resin. Under low salt condition and high negative SCD of resin used in their experiments, electrostatic interactions serve as the driving force for protein adsorption. In our simulation, when IS is low, protein adsorption is dominated by electrostatic interactions, which verifies the finding in experiments.[56,57] As the IS increases, back-on orientation becomes the preferred one. The binding sites of back-on orientation deviate from Lys1, Lys33, and Lys116 [Fig. 7(b)] because vdW interactions dominate protein adsorption and cannot be neglected in this case. For this orientation, the active site of lysozyme faces outward, which agrees well with the experimental results from Daly's work.[58] In their work, lysozyme is adsorbed on mica surfaces with its active site facing toward solution. Since mica surfaces are slightly negatively charged and hydrophilic, the orientation of adsorbed lysozyme is a compromise between electrostatic interactions and vdW interactions, which is the very case when IS increases to 0.1 or 0.3 M in our simulations. Therefore, it could be concluded that IS has significant effects on preferred orientations of lysozyme adsorbed on surfaces through the modulation of electrostatic interactions between lysozyme and surfaces. Moreover, from the phenomenon that orientation distribution is narrower at low IS where electrostatic interactions dominate, we concluded that an electrostatic-interaction-driven adsorption is favorable for positioning adsorbed protein layer in a uniform orientation, which confirms the electrostatically driven mechanism in controlling protein orientation proposed in our previous simulation work[25] for antibody orientation on charged surfaces.

Most other information of lysozyme orientations on surfaces in experiments is inferred from the height and mass of the adsorbed protein layer measured with instruments and the dimension of the protein. The dimensions or profiles of adsorbed lysozyme with the side-on and back-on orientations predicted in our simulations are consistent with that observed in experiments.[59,60] Robeson *et al.*[59] observed a hexagonal close-packed monolayer of horizontally oriented lysozyme molecules on negatively charged silica surfaces probed by total internal reflection fluorescence technique and scanning angle reflectometry method. Su *et al.*[60] found that lysozyme was adsorbed on a silica surface with side-on orientation by comparing the thickness of adsorbed lysozyme layer (calculated from the adsorbed lysozyme amount measured by neutron reflection) with lysozyme dimensions in x-, y-, and z-axis. Note that it is difficult to differentiate side-on and back-on orientations by experimentation because they have similar dimensions and profiles. Most experiments provide only some inferred information of orientations from dimensions or labeling sites of adsorbed proteins. However, our simulations directly provide a clear microscopic picture as well as the detailed binding information of protein adsorbed on surfaces.

As IS increases, the decrease in average total adsorption potential energy (Table I) indicates a decline in adsorbed amount. This phenomenon is also consistent with previous experimental[57,61–63] and theoretical results.[64] For example,

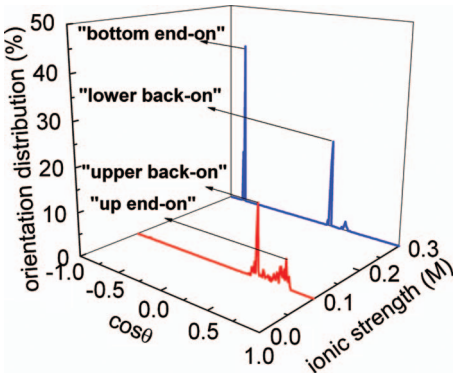

FIG. 8. Orientation distributions of lysozyme adsorbed on a positively charged surface at different ISs.

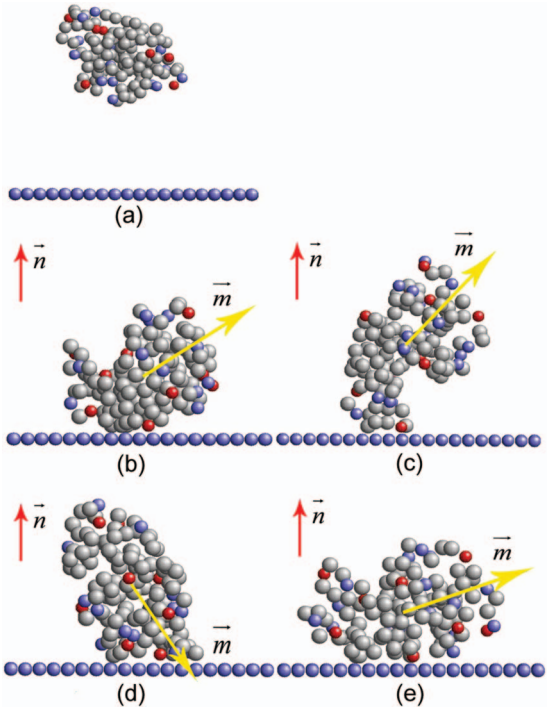

FIG. 9. Configurations of lysozyme orientation on a positively charged surface. The direction of normal to surface is noted as $\vec{n}$ and the direction of dipole of lysozyme is noted as $\vec{m}$. (a) No adsorption; (b) upper back-on orientation ($\cos\theta$=0.43); (c) up end-on orientation ($\cos\theta$=0.73); (d) bottom end-on orientation ($\cos\theta$=−0.81); (e) lower back-on orientation ($\cos\theta$=0.26).

Lewus *et al.*[61] investigated lysozyme adsorption and desorption behaviors on a silica surface and found that the equilibrium adsorbed amount decreases as the IS increases. Oberholzer and Lenhoff,[64] by calculating adsorption isotherms for small globular proteins in aqueous solution, found that IS had a strong effect on the behavior of protein adsorption and the electrostatic interactions were weakened as a result of an increase in IS.

C. Lysozyme orientation on a positively charged surface

The orientation distributions of adsorbed lysozyme on a positively charged surface (SCD=0.018 C m^{-2}) at different ISs are displayed in Fig. 8, corresponding configurations of possible orientations are shown in Fig. 9, and the potential energy of major orientations of adsorbed lysozyme is listed in Table II.

When IS is low (0.005 or 0.02 M), lysozyme is not adsorbed on the positively charged surface [Fig. 9(a)], which is consistent with experimental observation that positively charged microspheres do not adsorb lysozyme at neutral pH.[65] This can be explained by the strong repulsive electrostatic interactions (as indicated by the positive potential energy in Table II) between positively charged lysozyme and positively charged surface. As IS increases to 0.1 or 0.3 M, because of the increasing screening effect of ions from solution, lysozyme could be adsorbed on the positively charged surface with certain orientation distribution (Fig. 8). When IS=0.1 M, the "upper back-on" orientation with $\cos\theta$=0.46 [Fig. 9(b)] is preferred and the "up end-on" orientation with $\cos\theta$=0.73 [Fig. 9(c)] is also present. When IS=0.3 M, the "bottom end-on" orientation with $\cos\theta$=−0.81 [Fig. 9(d)] becomes the dominant orientation and the "lower back-on" orientation with $\cos\theta$=0.26 [Fig. 9(e)] still exists. From the potential energy contributed to lysozyme adsorption in Table II, it can be seen that despite of its net positive charge, lysozyme could be adsorbed on the like-charged surface with orientations having both attractive electrostatic and vdW interactions ("top end-on" and upper back-on orientations) or orientations having repulsive electrostatic interactions offset by attractive vdW interactions (bottom end-on and lower back-on orientations). Lysozyme adsorption on the like-charged surface is primarily a vdW-interaction-driven process when repulsive electrostatic interactions do not dominate. This phenomenon of charged protein adsorption on like-charged surfaces was reported in experimental studies,[66,67] indicating that protein adsorption behaviors on charged surfaces depend on not only the charge sign of protein and surface but also the discrete charge distribution over protein surface. Because of the nonuniform charge distribution over protein surface, local negatively charged sites of lysozyme may interact with positively charged surfaces. Moreover, IS plays an important role in protein adsorption through screening the repulsive electrostatic interactions. However, it is obvious that lysozyme adsorption is more favorable on negatively charged surfaces than on positively charged surfaces (as indicated by the adsorption potential energy listed in Tables I and II), which is in good agreement with experimental results that the negatively charged surface exhibits clearly faster adsorption and

TABLE II. Energies and orientations of lysozyme adsorbed on a positively charged surface.

IS (M)	U_{av} (kJ mol^{-1})	U_{tot} (kJ mol^{-1})	U_{vdW} (kJ mol^{-1})	U_{ele} (kJ mol^{-1})	cos θ	Orientation	P (%)	Fig.
0.005	15.6	15.6	0.0	15.6	⋯	⋯	⋯	9(a)
0.02	2.6	2.6	0.0	2.6	⋯	⋯	⋯	9(a)
0.1	−40.3	−40.8	−46.1	5.3	0.43	Upper back-on	91.47	9(b)
		−34.9	−26.6	−8.4	0.73	Top end-on	8.47	9(c)
		−22.5	−51.0	28.5	−0.81	Bottom end-on	0.06	8(d)
0.3		−60.3	−68.9	8.7	−0.81	Bottom end-on	62.07	9(d)
	−59.4	−58.7	−66.7	8.0	0.26	Lower back-on	33.23	9(e)
		−53.9	−49.0	−4.9	0.43	Upper back-on	4.70	9(b)

higher affinity for lysozyme than the positively charged surface.[48,68] The vdW-interaction-driven adsorption leads to a wider orientation distribution compared with electrostatic-interaction-driven adsorption, which is also found in our previous simulation study[25] that antibody exhibits multiple orientations when vdW interactions dominate.

IV. CONCLUSIONS

The PT MC algorithm is applied to probe the orientation of adsorbed proteins on surfaces. With this method, both lowest-energy orientation and orientation distribution could be acquired in a single simulation. Meanwhile, the coarse-grained united-residue model for proteins greatly reduces the degree of freedom of the simulated system and thus accelerates the simulation.

When applying the PTMC method to simulate lysozyme orientations on charged surfaces, it is found that when driven by dominant attractive electrostatic interactions, lysozyme tends to be adsorbed with side-on orientation on negatively charged surfaces. For this orientation, the active site faces sideways, and two binding sites are located around Lys1, Lys33, and Lys116, while Lys13, Lys96, and Lys97 are exposed to solution. With the contribution from vdW interactions increases, the preferred orientation changes to back-on orientation, which puts its active site outward. It is also found that despite of its net positive charge, lysozyme could be adsorbed on positively charged surfaces with both "end-on" and back-on orientations because of the nonuniform charge distribution over lysozyme surface and the screening effect from ions in solution. However, at low IS, lysozyme could not be adsorbed on positively charged surfaces because of too strong repulsive electrostatic interactions. These simulation results agree well with experimental data.

ACKNOWLEDGMENTS

This work is supported by the Program for New Century Excellent Talents in University (Grant No. NCET-07-0313) and the National Natural Science Foundation of China (Grant Nos. 20706019 and 20876052). The computational resources for this project are provided by SCUTGrid at South China University of Technology. We thank Michael Hague and Dr. Andrew Au for proofreading of the manuscript.

[1] B. Kasemo, Surf. Sci. **500**, 656 (2002).
[2] H. Nada and Y. Furukawa, J. Phys. Chem. B **112**, 7111 (2008).
[3] S. R. Raz, M. Bremer, M. Giesbers, and W. Norde, Biosens. Bioelectron. **24**, 552 (2008).
[4] D. Falkenhagen, W. Strobl, G. Vogt, A. Schrefl, I. Linsberger, F. J. Gerner, and M. Schoenhofen, Artif. Organs **23**, 81 (1999).
[5] A. J. Zhang, Y. Xie, and J. Zhou, Prog. Chem. **21**, 1408 (2009).
[6] F. Svec and J. M. Frechet, Science **273**, 205 (1996).
[7] B. D. Ratner, Biomaterials **28**, 5144 (2007).
[8] T. Sagara, Y. Kubo, and K. Hiraishi, J. Phys. Chem. B **110**, 16550 (2006).
[9] D. G. Myszka, J. Mol. Recognit. **12**, 279 (1999).
[10] J. L. Brash and T. A. Horbett, *Proteins at Interfaces 2*, ACS Symposium Series Vol. 602 (American Chemical Society, Washington, DC, 1995), p. 1.
[11] I. Szleifer, Biophys. J. **72**, 595 (1997).
[12] K. Nakanishi, T. Sakiyama, and K. Imamura, J. Biosci. Bioeng. **91**, 233 (2001).
[13] J. J. Gray, Curr. Opin. Struct. Biol. **14**, 110 (2004).
[14] P. Harder, M. Grunze, R. Dahint, G. M. Whitesides, and P. E. Laibinis, J. Phys. Chem. B **102**, 426 (1998).
[15] V. Castells, S. X. Yang, and P. R. Van Tassel, Phys. Rev. E **65**, 031912 (2002).
[16] A. M. Lenhoff, Langmuir **24**, 5991 (2008).
[17] R. W. Deitcher, Y. Xiao, J. P. O'Connell, and E. J. Fernandez, Biotechnol. Bioeng. **102**, 1416 (2009).
[18] G. Raffaini and F. Ganazzoli, Langmuir **20**, 3371 (2004).
[19] X. Chen, Q. Wang, J. W. Shen, H. H. Pan, and T. Wu, J. Phys. Chem. C **111**, 1284 (2007).
[20] M. Agashe, V. Raut, S. J. Stuart, and R. A. Latour, Langmuir **21**, 1103 (2005).
[21] B. Trzaskowski, F. Leonarski, A. Les, and L. Adamowicz, J. Phys. Chem. B **109**, 17734 (2005).
[22] J. Zhou, J. Zheng, and S. Y. Jiang, J. Phys. Chem. B **108**, 17418 (2004).
[23] J. Zheng, L. Y. Li, S. F. Chen, and S. Y. Jiang, Langmuir **20**, 8931 (2004).
[24] K. Wilson, S. J. Stuart, A. Garcia, and R. A. Latour, J. Biomed. Mater. Res. Part A **69A**, 686 (2004).
[25] J. Zhou, S. F. Chen, and S. Y. Jiang, Langmuir **19**, 3472 (2003).
[26] Y. Sun, W. J. Welsh, and R. A. Latour, Langmuir **21**, 5616 (2005).
[27] B. A. Berg and T. Neuhaus, Phys. Lett. B **267**, 249 (1991).
[28] A. P. Lyubartsev, A. A. Martsinovski, S. V. Shevkunov, and P. N. Vorontsov-Velyaminov, J. Chem. Phys. **96**, 1776 (1992).
[29] R. H. Swendsen and W. Jian-Sheng, Phys. Rev. Lett. **58**, 86 (1987).
[30] R. H. Swendsen and J. S. Wang, Phys. Rev. Lett. **57**, 2607 (1986).
[31] U. H. E. Hansmann, Chem. Phys. Lett. **281**, 140 (1997).
[32] D. J. Earl and M. W. Deem, Phys. Chem. Chem. Phys. **7**, 3910 (2005).
[33] Q. L. Yan and J. J. de Pablo, J. Chem. Phys. **111**, 9509 (1999).
[34] V. Ortiz, J. R. Maury-Evertsz, and G. E. Lopez, Chem. Phys. Lett. **368**, 452 (2003).
[35] R. Faller, Q. L. Yan, and J. J. de Pablo, J. Chem. Phys. **116**, 5419 (2002).
[36] H. Fukunishi, O. Watanabe, and S. Takada, J. Chem. Phys. **116**, 9058 (2002).
[37] N. Rathore and J. J. de Pablo, J. Chem. Phys. **116**, 7225 (2002).
[38] N. Rathore, T. A. Knotts, and J. J. de Pablo, Biophys. J. **85**, 3963 (2003).
[39] N. Rathore, T. A. Knotts, and J. J. de Pablo, J. Chem. Phys. **118**, 4285 (2003).
[40] T. A. Knotts, N. Rathore, and J. J. de Pablo, Proteins: Struct., Funct., Bioinf. **61**, 385 (2005).
[41] T. A. Knotts, N. Rathore, and J. J. de Pablo, Biophys. J. **94**, 4473 (2008).
[42] A. Liwo, S. Oldziej, M. R. Pincus, R. J. Wawak, S. Rackovsky, and H. A. Scheraga, J. Comput. Chem. **18**, 849 (1997).
[43] J. Zhou, I. F. Thorpe, S. Izvekov, and G. A. Voth, Biophys. J. **92**, 4289 (2007).
[44] F. Wang, S. J. Stuart, and R. A. Latour, BioInterphases **3**, 9 (2008).
[45] F. Galisteo and W. Norde, Colloids Surf., B **4**, 389 (1995).
[46] J. R. Lu, X. B. Zhao, and M. Yaseen, Curr. Opin. Colloid Interface Sci. **12**, 9 (2007).
[47] D. T. Kim, H. W. Blanch, and C. J. Radke, Langmuir **18**, 5841 (2002).
[48] K. Rezwan, L. P. Meier, and L. J. Gauckler, Biomaterials **26**, 4351 (2005).
[49] W. Feng, S. P. Zhu, K. Ishihara, and J. L. Brash, Langmuir **21**, 5980 (2005).
[50] H. K. Tsao, J. Colloid Interface Sci. **202**, 527 (1998).
[51] D. A. Kofke, J. Chem. Phys. **117**, 6911 (2002).
[52] N. Rathore, M. Chopra, and J. J. de Pablo, J. Chem. Phys. **122**, 024111 (2005).
[53] A. Kone and D. A. Kofke, J. Chem. Phys. **122**, 206101 (2005).
[54] J. Zhou, H. K. Tsao, Y. J. Sheng, and S. Y. Jiang, J. Chem. Phys. **121**, 1050 (2004).
[55] S. F. Chen, L. Y. Liu, J. Zhou, and S. Y. Jiang, Langmuir **19**, 2859 (2003).
[56] F. Dismer and J. Hubbuch, J. Chromatogr. A **1149**, 312 (2007).
[57] F. Dismer, M. Petzold, and J. Hubbuch, J. Chromatogr. A **1194**, 11 (2008).
[58] S. M. Daly, T. M. Przybycien, and R. D. Tilton, Langmuir **19**, 3848 (2003).

[59] J. L. Robeson and R. D. Tilton, Langmuir **12**, 6104 (1996).
[60] T. J. Su, J. R. Lu, R. K. Thomas, Z. F. Cui, and J. Penfold, Langmuir **14**, 438 (1998).
[61] R. K. Lewus, F. H. Altan, and G. Carta, Ind. Eng. Chem. Res. **37**, 1079 (1998).
[62] Q. L. Luo and J. D. Andrade, J. Colloid Interface Sci. **200**, 104 (1998).
[63] R. E. Holmlin, X. X. Chen, R. G. Chapman, S. Takayama, and G. M. Whitesides, Langmuir **17**, 2841 (2001).
[64] M. R. Oberholzer and A. M. Lenhoff, Langmuir **15**, 3905 (1999).
[65] S. R. Van Tomme, B. G. De Geest, K. Braeckmans, S. C. De Smedt, F. Siepmann, J. Siepmann, C. F. van Nostrum, and W. E. Hennink, J. Controlled Release **110**, 67 (2005).
[66] C. A. Haynes, E. Sliwinsky, and W. Norde, J. Colloid Interface Sci. **164**, 394 (1994).
[67] T. Zoungrana, G. H. Findenegg, and W. Norde, J. Colloid Interface Sci. **190**, 437 (1997).
[68] X. Q. Wang, H. L. Sun, Y. Q. Xia, C. X. Chen, H. Xu, H. H. Shan, and J. R. Lu, J. Colloid Interface Sci. **332**, 96 (2009).